Noninvasive diagnosis of pulmonary hypertension with hyperpolarised ^{129}Xe magnetic resonance imaging and spectroscopy

Elianna A. Bier[1], Fawaz Alenezi[2], Junlan Lu[3], Ziyi Wang[1], Joseph G. Mammarappallil[4], Bryan O'Sullivan-Murphy[4], Alaattin Erkanli[5], Bastiaan Driehuys[4] and Sudarshan Rajagopal[2]

[1]Dept of Biomedical Engineering, Duke University, Durham, NC, USA. [2]Division of Cardiology, Department of Medicine, Duke University Medical Center, Durham, NC, USA. [3]Medical Physics Graduate Program, Duke University, Durham, NC, USA. [4]Dept of Radiology, Duke University Medical Center, Durham, NC, USA. [5]Dept of Biostatistics and Bioinformatics, Duke University, Durham, NC, USA.

Corresponding author: Sudarshan Rajagopal (sudarshan.rajagopal@duke.edu)

Shareable abstract (@ERSpublications)
Diagnostic models using ^{129}Xe MRI/MRS metrics can noninvasively detect pre-capillary PH, post-capillary PH and ILD. The combination of ^{129}Xe MRI/MRS provides a comprehensive assessment of haemodynamics and gas-exchange impairment in individual patients. https://bit.ly/3tDJw5P

Cite this article as: Bier EA, Alenezi F, Lu J, *et al*. Noninvasive diagnosis of pulmonary hypertension with hyperpolarised ^{129}Xe magnetic resonance imaging and spectroscopy. *ERJ Open Res* 2022; 8: 00035-2022 [DOI: 10.1183/23120541.00035-2022].

Received: 19 Jan 2022
Accepted: 10 March 2022

Abstract

Background The diagnosis of pulmonary hypertension (PH) remains challenging. Pre- and post-capillary PH have different signatures on noninvasive ^{129}Xe gas-exchange magnetic resonance imaging (MRI) and dynamic MR spectroscopy (MRS). We tested the accuracy of ^{129}Xe MRI/MRS to diagnose PH status compared to right heart catheterisation (RHC).

Methods ^{129}Xe MRI/MRS from 93 subjects was used to develop a diagnostic algorithm, which was tested in 32 patients undergoing RHC on the same day (n=20) or within 5 months (42±40 days) (n=12). Three expert readers, blinded to RHC, used ^{129}Xe MRI/MRS to classify subjects as pre-capillary PH, post-capillary PH, no PH and no interstitial lung disease (ILD), or ILD.

Results For pre-capillary PH, ^{129}Xe MRI/MRS diagnostic accuracy was 75% (95% CI 66–84) with a sensitivity of 67% (95% CI 54–79) and a specificity of 86% (95% CI 75–96); for post-capillary PH accuracy was 69% (95% CI 59–78) with sensitivity of 54% (95% CI 34–74) and specificity of 74% (95% CI 63–84). The model performed well in straightforward cases of pre-capillary PH but was less accurate in its diagnosis in the presence of mixed disease, particularly in the presence of ILD or combined post- and pre-capillary PH.

Conclusion This study demonstrates the potential to develop ^{129}Xe MRI/MRS into a modality with good accuracy in detecting pre- and post-capillary PH. Furthermore, the combination of ^{129}Xe dynamic MRS and gas-exchange MRI uniquely provide concurrent, noninvasive assessment of both haemodynamics and gas-exchange impairment that may aid in the detection of PH.

Introduction

Hyperpolarised ^{129}Xe gas-exchange magnetic resonance imaging/MR spectroscopy (^{129}Xe MRI/MRS) is a rapid and noninvasive tool with significant potential to evaluate a variety of debilitating pulmonary pathologies [1–3]. ^{129}Xe, once inhaled, freely diffuses from the airspaces, across the interstitial barrier tissues, and into the pulmonary capillaries, with distinct spectral peaks in each of these compartments [4]. In a single breath-hold, this enables separate imaging and spectral characterisation of the ventilated ^{129}Xe distribution in the airspaces, its uptake in lung parenchyma and blood plasma (referred to collectively as barrier), and transfer to red blood cells (RBCs) [5]. These 3D images are transformed into quantitative maps that report on the severity and spatial heterogeneity of pulmonary disease as it affects the airspace, interstitial and pulmonary vascular compartments. Such imaging can be coupled with ^{129}Xe dynamic MRS [6–8], which reveals cardiogenic variations of ^{129}Xe transfer to the capillary RBCs that can differentiate

pre- and post-capillary pulmonary hypertension (PH) [9]. Through these unique properties, ^{129}Xe MRI reports both on pulmonary gas exchange and variation in capillary blood volume, providing a detailed assessment of lung disease as well as the potential presence of pre- or post-capillary PH.

PH lacks specific symptoms and is thus frequently attributed to other common heart and lung conditions, resulting in a delay of clinical suspicion [10]. The diagnosis and follow-up of patients with PH is challenging, with an absence of unambiguous biomarkers that reflect the underlying complexity of its pathophysiology [11]. PH is caused by a variety of conditions, which has led to its classification into five clinical groups: pulmonary arterial hypertension (PAH – Group 1 PH), PH due to left heart disease (Group 2 PH), PH due to chronic lung disease (Group 3), PH due to pulmonary vascular obstruction (Group 4) and PH due to miscellaneous causes (Group 5) [12]. For example, a common problem in PH diagnosis is the differentiation between pre-capillary, isolated post-capillary (IpcPH) and combined pre- and post-capillary PH (CpcPH), which are frequently based on population-based "normal" values that do not reflect patient-specific physiology related to age or concomitant heart and lung disease [13]. Thus, there remains an unmet need for tools that can differentiate between different PH phenotypes and allow proper classification and risk stratification to guide therapy and monitor disease progression.

The unique properties of ^{129}Xe MRI have the potential to address a significant remaining unmet clinical need for noninvasive diagnostic testing in PH. Recently we identified ^{129}Xe MRI signatures that differentiate between patients with COPD, idiopathic pulmonary fibrosis, pre-capillary PH (PAH) and post-capillary PH (left heart disease) [9]. That finding suggested that ^{129}Xe MRI could be used to screen for or diagnose pre-capillary PH and differentiate it from other common cardiopulmonary disease. Here, we used those signatures to develop a diagnostic algorithm for the detection of pre-capillary PH IpcPH and interstitial lung disease (ILD) and validated it in an independent cohort of patients who underwent contemporaneous ^{129}Xe MRI/MRS and right heart catheterisation (RHC).

Methods

Subject recruitment

This study was approved by the Institutional Review Board of Duke University Medical Center. Written informed consent was obtained from each subject prior to recruitment.

A training cohort of 93 subjects (no PH n=38, pre-capillary PH n=22, post-capillary PH n=9, ILD without known PH n=24) was used to construct the diagnostic algorithm. These subjects had been scanned under prior study protocols, in which ^{129}Xe MR gas-exchange images and ^{129}Xe dynamic spectra were acquired using the standard parameters described below [5, 6, 9, 14, 15].

The test cohort consisted of 32 subjects (mean age, 58±15 years; 19 women) that were undergoing RHC for the evaluation of dyspnoea. RHC was performed on the same day (n=20) or within 5 months (42±40 days) (n=12) of ^{129}Xe MRI/MRS and was used as the gold standard to determine PH status (no PH, pre-capillary, IpcPH or CpcPH) (see below for haemodynamic definitions used for each).

^{129}Xe gas hyperpolarisation and MR imaging and spectroscopy acquisition

^{129}Xe was hyperpolarised *via* continuous flow spin exchange optical pumping and cryogenic accumulation using commercially available systems (Model 9820 and 9810; Polarean plc., Durham, NC, USA) and dispensed into a Tedlar™ dose delivery bag [16]. For MRS the dispensed gas had a ^{129}Xe dose equivalent of 64±20 mL (polarisation=20.8±7.5%; xenon volume=380±69 mL), while for MRI it was 159±43 mL (polarisation=28.5±8.8%; xenon volume 676±52 mL) [16]. Both bags were expanded to the desired total inhalation volume using the xenon flow gas blend (1% Xe/10% N_2/89% He). 28 subjects received a standard total gas volume of 1 L, while four subjects received a gas volume tailored to 20% of their forced vital capacity (FVC) as per the recent recommended guidelines [17]. Thus, the mean gas volume delivered across the 32 subjects was 954±152 mL. ^{129}Xe spectroscopy and imaging were acquired on either a 1.5 T (GE 15M4 EXCITE (GE Healthcare, Waukesha, WI, USA), training cohort) or a 3 T (SIEMENS MAGNETOM Trio (Siemens, Erlangen, Germany), training and testing cohort) scanner during two separate breath-holds of ^{129}Xe [17]. For each scan, subjects were coached to inhale the ^{129}Xe from functional residual capacity (FRC).

Subjects first underwent dynamic MRS during which ^{129}Xe free induction decays (FIDs) were collected every 15 or 20 ms (TE=0.932 ms, flip angle ≈20°, dwell time=32 µs, 512/1024 points) during an 8–16 s breath-hold [6]. This flip angle and repetition time (TR) combination corresponded to an effective TR of ∼332 or 249 ms [18], ensuring that the observed signal arose from the pulmonary capillary bed. 3D images were then acquired using an interleaved radial acquisition of gas- and dissolved-phase signal during

a 15 s breath-hold [5]. The signal was acquired at an echo time that allowed the barrier and RBC dissolved-phase compartments to be decomposed using the 1-point Dixon method [19]. These data were reconstructed at 6 mm isotropic resolution to provide 3D images of the gas, barrier and RBC signal distributions. For each subject complete ^{129}Xe MRI/MRS required ∼30 min including patient positioning, breath coaching and a proton image for an anatomical reference.

Quantitative processing and analysis

Quantitative processing of the spectroscopy acquisition followed the procedure detailed in [6] and is briefly summarised here. FIDs from ^{129}Xe dynamic MRS were fit in the time domain to a barrier Voigt model [6] to determine static ratio RBC:barrier, RBC chemical shift and the cardiogenic variation in the RBC signal amplitude. These oscillations were quantified by their peak-to-peak height relative to the mean and compared to typical values found in a healthy reference population [6]. For the test cohort, the signal-to-noise ratio (SNR) of the static RBC peak was 45±27.

Gas-exchange images were transformed into quantitative maps depicting ^{129}Xe ventilation, and barrier tissue uptake and RBC transfer relative to the gas signal. Each of these maps were quantified by calculating the percentage of the lung exhibiting signal defects, low, normal and high signal with respect to a healthy reference population [15]. Note that barrier and RBC signal can only arise from regions that are ventilated and actively participating in gas exchange. Thus, barrier and RBC quantitative analysis excludes regions containing ventilation defects.

Diagnostic algorithm development

The diagnostic algorithm was created using the 93-subject training cohort. To evaluate which imaging and spectroscopy parameters were the best predictors of PH or ILD status, we employed predictor screening using a bootstrapped decision-tree algorithm [20, 21]. The highest-ranking predictor of PH status was found to be the RBC signal oscillation amplitude, followed by RBC:barrier ratio and RBC defect percentage. Thus, the RBC oscillation amplitudes were used as the first step of the algorithm, assigning them to five initial classes: pre-capillary PH, possible pre-capillary PH, no PH, possible IpcPH or ILD, and IpcPH or ILD. This process used thresholds that were determined using receiver operating characteristics (ROC), with strict cut-offs for pre-capillary PH or IpcPH, and a softer cut-off to differentiate possible pre-capillary PH or IpcPH from normal. The strict cut-offs were determined by requiring high specificity of >90% to reduce the number of false positives. The soft cut-offs were determined using a more modest 85% sensitivity to reduce the number of false negatives. For cases classified as possible pre-capillary PH or IpcPH, the presence of RBC transfer impairment was used to verify these classifications or whether they should be listed as normal. For this test, both RBC defect alone and the sum of RBC defect+low percentages were evaluated for predictive performance; RBC defect+low was found to have a higher ROC area under the curve for correctly classifying the training subjects. The RBC defect+low limit was optimised on the potential pre-capillary PH and IpcPH subjects to best classify those with PH *versus* those without. Finally, we sought to separate IpcPH from ILD, as both of these groups exhibited high RBC oscillations and RBC transfer impairments [9]. Here, we employed prior findings that ILD subjects exhibit high interstitial barrier uptake on imaging [22, 23], and a low RBC chemical shift on spectroscopy, indicative of delayed capillary blood oxygenation [8]. Requiring the presence of both of these traits was found, within the training cohort, to most accurately classify subjects as having ILD *versus* IpcPH.

Testing diagnostic algorithm performance

The algorithm performance for detecting PH was tested using a cohort of 32 patients who underwent both ^{129}Xe MRI/MRS and RHC. The patient's definite PH status (no PH, pre-capillary, IpcPH or CpcPH) was determined based on RHC measurements of mean pulmonary artery pressure (mPAP), pulmonary capillary wedge pressure (PCWP) and pulmonary vascular resistance (PVR). A diagnosis of PH was established from mPAP $\geqslant$20 mmHg, while pre-capillary PH required PCWP $\leqslant$15 mmHg and PVR $\geqslant$3 Wood Units (WU), and IpcPH required PCWP >15 mmHg and PVR <3 WU [6, 24]. Patients presenting with both high PVR and PCWP >15 mmHg were classified as CpcPH [25]. To test algorithm performance, subjects with CpcPH were treated as positive for both pre- capillary PH and IpcPH, and subjects with PH that was neither pre-capillary nor post-capillary were treated as negative for both pre- and IpcPH.

Three expert readers (cardiothoracic radiologists), blinded to the RHC findings and medical histories, were trained to interpret ^{129}Xe MRI/MRS and apply the diagnostic algorithm. Readers were asked to classify each subject as either pre-capillary PH, IpcPH, no PH and no ILD, or ILD. They were further asked to rate the diagnostic quality of the scans for each subject and report if ^{129}Xe gas-exchange imaging indicated the presence of other restrictive or obstructive pulmonary disease. Trained readers could review each case and assign a PH category in under 5 min.

Separate performance statistics were calculated for each possible reader classification. In addition, performance statistics were determined for the combined category of IpcPH and ILD, since both are associated with enhanced RBC amplitude oscillations.

Statistical testing

All statistical processing was performed using JMP version 15 (SAS Institute, Cary, NC, USA). Algorithm performance was quantified by the sensitivity, specificity, positive predictive value (PPV), negative predictive value (NPV) and diagnostic accuracy. Inter-rater agreement was assessed using Fleiss' kappa coefficient.

Results

Diagnostic algorithm

Figure 1 displays example ^{129}Xe MRI/MRS results for representative subjects in the training cohort. The healthy volunteer exhibits RBC amplitude oscillations of 10.5% within the published healthy reference range (median (IQR) 9.2% (8.1–11.6) [9] as well as a static RBC chemical shift of 218.5 ppm, also within reference (median (IQR) 218.2 ppm (217.9–218.6) [22]. In this subject, ventilation, barrier and RBC transfer images fall largely into the normal (green) range. The PAH subject (pre-capillary PH) has diminished RBC amplitude oscillations due to occlusion upstream of the capillary bed, and a normal ventilation pattern with moderate RBC transfer impairment (red and orange). The post-capillary PH subject has enhanced RBC oscillations due to impedance downstream of the pulmonary capillaries with a normal ventilation pattern and moderate RBC transfer impairment. The ILD subject also has enhanced amplitude oscillations, thought to result from a preserved cardiac output feeding into a capillary volume that has been decreased by fibrosis [6], along with a reduced RBC chemical shift, and a high (purple) barrier uptake.

^{129}Xe MRI/MRS results from the 93 subjects in the training cohort were used as described in the section Diagnostic algorithm development to create the diagnostic algorithm summarised in figure 2. First, the RBC signal oscillation amplitude is evaluated to determine the possible presence of PH and, if so, whether it is pre- (<8.6%) or post-capillary (>11.0%). For equivocal cases of possible PH, the additional presence of large regions of defect+low RBC transfer (>30%) confirms PH on both the pre- and post-capillary branches. And finally, IpcPH is differentiated from ILD by testing for presence of enhanced barrier uptake (>25%) and low RBC shift (<217 ppm). Note, however, that this algorithm is unable to identify CpcPH, PH that is neither pre- nor post-capillary, or PH in the presence of ILD.

Test cohort

Table 1 lists the key characteristics of the 32-subject test cohort, including demographics and RHC-derived haemodynamic indices. In the test cohort, RHC indicated that 15 subjects had pre-capillary PH, five had IpcPH, three had CpcPH, two had PH that was neither pre- nor post-capillary, and seven had no PH. Seven of the 32 subjects in the test cohort had a clinical history of ILD, of which four also had PH (two pre-capillary PH, one IpcPH, one PH that was neither pre- nor post-capillary).

Reader study and algorithm performance

When testing the diagnostic accuracy of ^{129}Xe MRI/MRS relative to RHC, Reader 1 properly classified 19 subjects, while Reader 2 properly classified 18 and Reader 3 properly classified 21 subjects. There were six subjects misclassified by all three readers; two of these subjects presented with PH that was neither pre- nor post-capillary, a category the model cannot detect. The majority of subjects with CpcPH were classified by readers as pre-capillary PH. Full diagnostic performance statistics are presented in table 2.

For the detection of pre-capillary PH, the algorithm had a diagnostic accuracy of 75% (95% CI 66–84) with a sensitivity of 67% (95% CI 54–79) and a specificity of 86% (95% CI 75–96). This was reflected in a PPV of 86% (95% CI 75–96) and a NPV of 67% (95% CI 54–79). To assess reader agreement on the determination of pre-capillary PH, Fleiss' kappa coefficient was calculated with κ=0.70 indicating good agreement between readers.

The detection of IpcPH had a diagnostic accuracy of 69% with a sensitivity of 54% (95% CI 34–74) and a specificity of 74% (95% CI 63–84). Similarly, the detection of ILD has a diagnostic accuracy of 78% (95% CI 70–86) with a sensitivity of 29% (95% CI 9–48) and a specificity of 92% (95% CI 86–98). However, the combined category of IpcPH or ILD had the highest diagnostic accuracy at 77% (95% CI 69–85) and the highest sensitivity at 76% (95% CI 63–89) and a specificity of 78% (95% CI 67–89). Thus, the diagnostic algorithm could identify IpcPH or ILD but was unable to accurately differentiate the two. A *post hoc* test excluding subjects with known ILD did not materially improve performance.

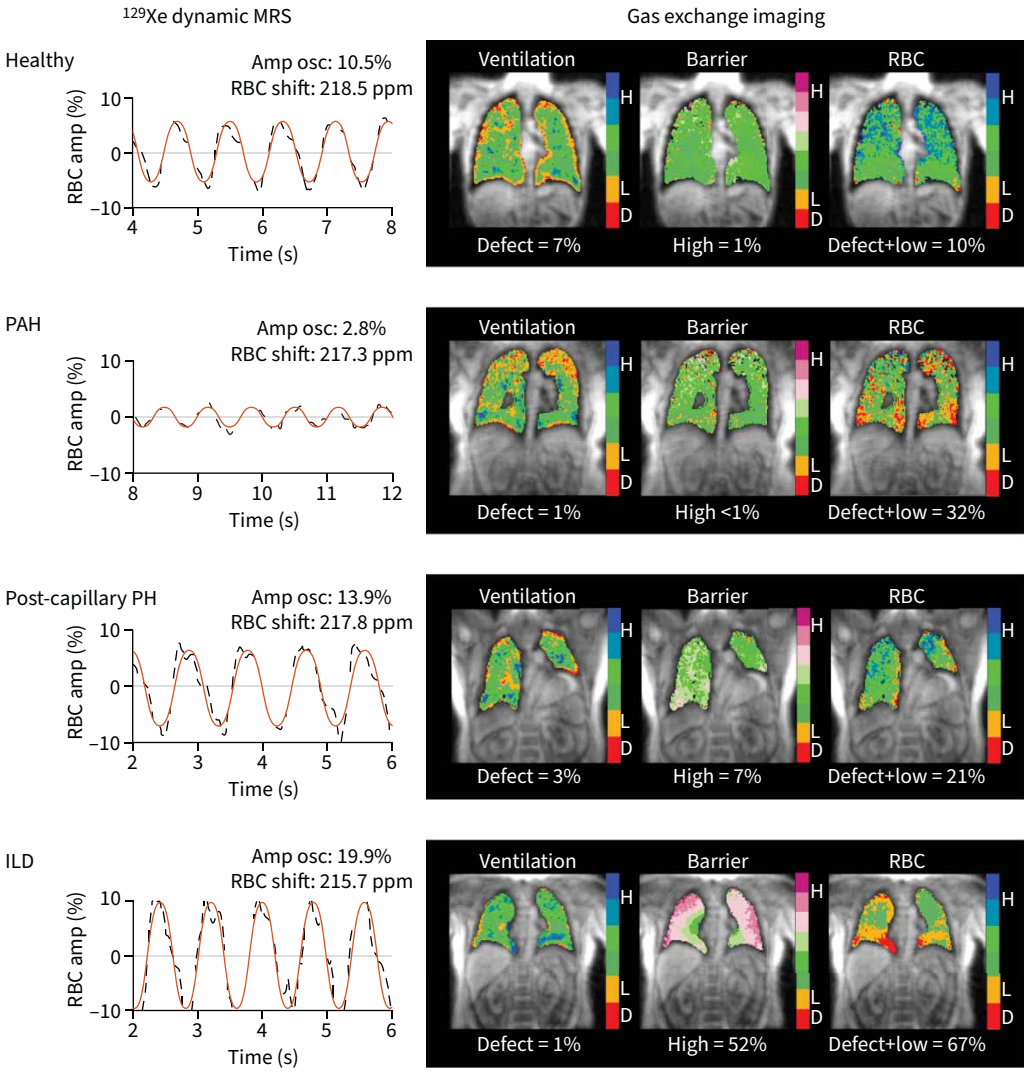

FIGURE 1 Representative ^{129}Xe gas-exchange magnetic resonance imaging/MR spectroscopy (^{129}Xe MRI/MRS) for subjects used to develop the ^{129}Xe diagnostic model. The displayed results for each subject include the red blood cell (RBC) oscillation amplitude and static RBC chemical shift from ^{129}Xe dynamic MRS, and quantitative maps depicting ^{129}Xe ventilation, barrier tissue uptake and RBC transfer relative to the gas signal. The ventilation is quantified by the percentage of the lung with signal defects (red) relative to a healthy population. The barrier uptake is quantified by the percentage of lung with high signal (purple) relative to a healthy reference population. RBC transfer is quantified by the sum of the percentage of lung with signal defects (red) and low signal (orange) (defect+low). amp: amplitude; amp osc: amplitude oscillations; PH: pulmonary hypertension; PAH: pre-capillary PH; ILD: interstitial lung disease.

Pre-capillary PH: ^{129}Xe MRI/MRS correct classifications

It is instructive to review several cases from the test cohort to illustrate when the ^{129}Xe MRI/MRS diagnostic algorithm had both good and poor performance. Figure 3 contains the ^{129}Xe MRI/MRS results from three subjects that were classified correctly by every reader as pre-capillary PH. The diagnostic algorithm performed well on straightforward cases such as these. Each subject exhibited reduced RBC amplitude oscillations, with low to moderate ventilation defects, normal barrier uptake and moderately reduced RBC transfer. The corresponding haemodynamic measurements for each subject revealed significantly elevated mPAP, indicating more severe disease.

Pre-capillary PH: ^{129}Xe MRI/MRS misclassifications

Figure 4 contains three examples of subjects with PH that were misclassified by at least two of the three readers. Subject Test-10 exhibited RBC oscillations in the normal range and was misclassified by two

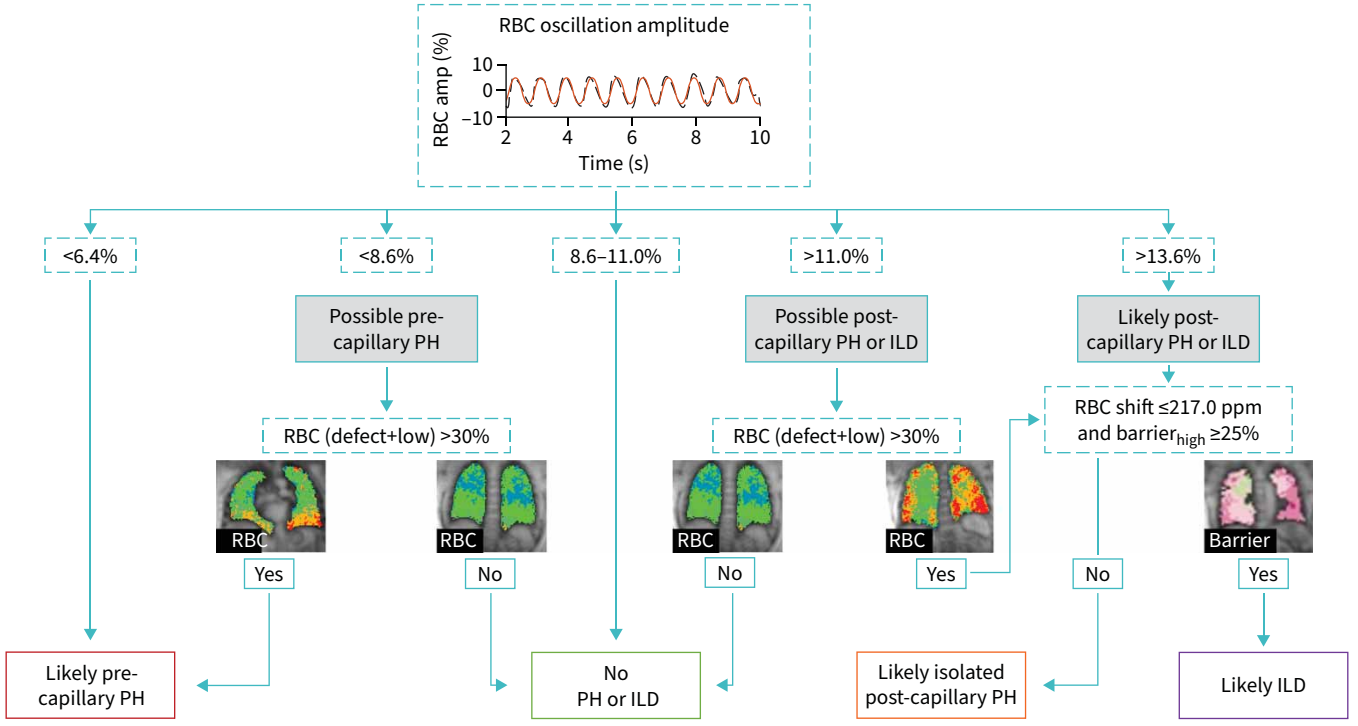

FIGURE 2 Baseline diagnostic algorithm for determining pre- *versus* post-capillary pulmonary hypertension (PH) based on ^{129}Xe red blood cell (RBC) oscillation amplitude (amp) and gas-exchange images. ILD: interstitial lung disease.

readers as having no PH while RHC indicates mild PH. However, gas-exchange imaging showed that the subject had severe obstructive lung disease, suggesting PH may be proportionate to lung disease. Subject Test-24 exhibited normal RBC oscillations and was thus misclassified by all three readers as having no PH. However, this subject had both elevated mPAP and PVR that indicate pre-capillary PH, but again had substantial ventilation defects and mildly elevated barrier. This subject had a clinical diagnosis of asthma combined with pre-capillary PH. Subject Test-03 exhibited small RBC oscillations and was also misclassified by all three readers as pre-capillary PH. However, this subject had a PVR just under 3.0 WU, and thus was classified by RHC as neither pre- nor post-capillary PH. Note that this patient would be considered to have an elevated PVR based on a recent population-based study [26]. Moreover, they were found to have chronic thromboembolic disease, which was successfully treated by pulmonary endarterectomy.

Mixed disease: CpcPH and PH in the setting of chronic lung disease

Figure 5 illustrates examples of mixed disease. Subject Test-02 had CpcPH but was classified by two readers as having pre-capillary PH and by one reader as IpcPH. Although RBC amplitude oscillations fell within the normal range, the readers used the high degree of RBC transfer impairment to classify the subject as having PH. Indeed, RHC revealed high mPAP, indicative of severe PH, but the combination of both high PCWP and PVR classified the subject as CpcPH. A similar misclassification is seen in Subject Test-18, where the subject exhibited a normal RBC oscillation amplitude with a low RBC chemical shift on MRS with high barrier uptake on MRI. These ^{129}Xe MRI/MRS findings are consistent with ILD; however, RHC indices show this subject also has pre-capillary PH. Subject Test-32 had enhanced oscillations with preserved chemical shift and high barrier uptake. With the exception of the preserved chemical shift, these findings are again consistent with ILD. However, RHC indices show the subject to have mild PH, with normal wedge pressure and elevated PVR, suggesting pre-capillary PH.

Discussion

The current diagnostic approach for PH relies on both invasive and noninvasive studies that can remain difficult to interpret in patients with concomitant cardiopulmonary disease. Therefore, it is critical to develop additional noninvasive approaches to detect PH, determine whether it is pre- or post-capillary, and evaluate concomitant lung disease. Although pulmonary function testing with diffusing capacity of the

TABLE 1 Demographic and clinical characteristics stratified by PH status

Characteristic	PrePH	IpcPH	CpcPH	PH (not pre or post)	No PH
Subjects n	15	5	3	2	7
Age	55 (51–62)	62 (65–73)	66 (62–70)	58 (58–58)	54 (40–70)
Female sex n	7	2	3	1	6
Race n					
White	9	4	3	2	7
Black	5	0	0	0	0
Smoker n	4	2	1	2	1
WHO functional class n					
Class 1	2	2	2	2	0
Class 2	8	3	0	0	5
Class 3	3	0	1	0	2
Class 4	1	0	0	0	0
Medications n					
PDE5 inhibitor	1	0	1	0	1
Endothelin receptor antagonist	6	0	0	0	0
Pulmonary function tests					
FEV_1 % pred	57 (42–71)	63 (51–68)	68 (66–71)	82 (75–88)	92 (54–110)
FVC % pred	66 (57–75)	67 (50–72)	78 (76–81)	86 (73–99)	86 (53–113)
FEV_1/FVC %	84 (78–96)	102 (101–104)	85 (80–90)	100 (92–107)	79 (74–106)
TLC % pred	83 (72–91)	79 (60–90)	83 (80–88)	114 (114–114)	123 (114–132)
D_{LCO} % pred	55 (32–75)	75 (69–88)	67 (61–73)	83 (61–104)	84 (40–128)
Invasive haemodynamics (RHC)					
Cardiac index $L \cdot min^{-1} \cdot m^{-2}$	2.9 (2.4–2.8)	2.7 (2.5–2.8)	2.2 (2.0–2.4)	2.9 (2.4–3.5)	3.1 (2.6–3.7)
RA pressure mmHg	9 (6–11)	10 (8–12)	12 (12–12)	6 (6–6)	4.5 (3.0–6.0)
PCWP mmHg	12 (10–14)	18 (16–19)	18 (17–19)	12 (10–13)	10 (9–12)
PA mean pressure mmHg	41 (34–48)	29 (25–32)	49 (46–52)	26 (25–27)	17 (15–19)
PVR Wood units	5.6 (4.3–6.9)	1.8 (1.2–2.2)	7.6 (6.5–8.3)	2.6 (2.4–2.7)	1.1 (0.6–1.5)
Echocardiographic parameters					
LV ejection fraction %	61 (60–65)	62 (60–65)	63 (63–65)	58 (56–59)	53 (45–60)
Tricuspid regurgitation n					
0 – trivial	2	2	2	2	0
1 – mild	8	3	0	0	4
2 – moderate	3	0	1	0	3
3 – severe	1	0	0	0	0
TAPSE cm	2.0 (1.6–2.7)	2.7 (2.3–2.7)	1.5 (1.4–1.7)	2.5 (2.4–2.6)	1.6 (1.4–1.8)
RVSP mmHg	52 (36–67)	35 (29–41)	56 (47–72)	15 (15–15)	20 (15–25)
Resting heart rate	71 (69–81)	74 (68–83)	79 (74–83)	83 (81–84)	83 (74–88)

Data are either presented as number of participants or as median (IQR) where the first number in parentheses is the first quartile and the second number in parentheses is the third quartile. One prePH subject and one no PH subject did not have echocardiography results and are omitted from echocardiographic parameters. PH: pulmonary hypertension; PrePH: pre-capillary PH; IcpPH: isolated post-capillary PH; CpcPH: combined post- and pre-capillary PH; WHO: World Health Organisation; FEV_1 % pred: percentage of predicted forced expiratory volume in 1 s; FVC % pred: percentage of predicted forced vital capacity; TLC % pred: percentage of predicted total lung capacity; D_{LCO} % pred: percentage of predicated diffusing capacity of the lung for carbon monoxide; RHC: right heart catheterisation; RA: right atrial; PCWP: pulmonary capillary wedge pressure; PA: pulmonary artery; PVR: pulmonary vascular resistance; LV: left ventricular; TAPSE: tricuspid annular plane systolic excursion; RVSP: right ventricular systolic pressure.

lung for carbon monoxide (D_{LCO}) can identify alterations in pulmonary gas exchange that are associated with PH, this is of limited utility in diagnosis as it provides only an indirect readout of impairment occurring within the pulmonary microvasculature [27, 28]. Thus, PH diagnosis and monitoring continues to rely on measuring increases in PVR and PAP or changes in right ventricular function [29]. To this end, RHC remains the diagnostic gold standard for PH based on a definition of a mPAP of >20 mmHg. However, such elevated pressures can arise from a wide variety of underlying causes (Groups 1–5), which RHC does not readily differentiate. RHC has additional limitations, such as its invasive nature and the effects of sedation and cardiopulmonary comorbidities on its measurement, which affect its accuracy and interpretation [12]. As a result, PH screening and progression monitoring employs echocardiography [30], which is noninvasive, widely available and relatively inexpensive. However, potential limitations include the weak correlation and diagnostic accuracy in patients with high pulmonary pressures, inability to acquire an estimate of systolic PAP in certain patient populations (*i.e.* COPD) and underestimation when the tricuspid regurgitant jet is of insufficient quality [31]. Given these remaining challenges, and that ^{129}Xe

TABLE 2 Diagnostic algorithm performance statistics with 95% confidence intervals

Reader classification	PrePH	IpcPH	No PH and no ILD	ILD	IpcPH or ILD
Subjects n	18	8	4	7	14
Prevalence %	56	25	13	22	44
Fleiss' kappa	0.70	0.48	−0.05	0.05	0.71
Sensitivity	67 (54–79)	54 (34–74)	25 (1–50)	29 (9–48)	76 (63–89)
Specificity	86 (75–96)	74 (63–84)	89 (83–96)	92 (86–98)	78 (67–89)
PPV	86 (75–96)	41 (24–58)	25 (1–50)	50 (22–78)	73 (60–86)
NPV	67 (54–79)	83 (74–92)	89 (83–96)	82 (74–90)	81 (70–91)
Diagnostic accuracy	75 (66–84)	69 (59–78)	81 (73–89)	78 (70–86)	77 (69–85)

Data are percentages with 95% confidence interval presented in parentheses, unless indicated otherwise. PH: pulmonary hypertension; PrePH: pre-capillary PH; IcpPH: isolated post-capillary PH; ILD: interstitial lung disease; PPV: positive predictive value; NPV: negative predictive value.

MRI/MRS is a well-tolerated and noninvasive method that reports on both pulmonary capillary haemodynamics and gas-exchange abnormalities. It has the potential to address these current limitations in PH diagnosis either as a stand-alone exam or alongside traditional diagnostic methods to provide orthogonal information that can aid in disease classification.

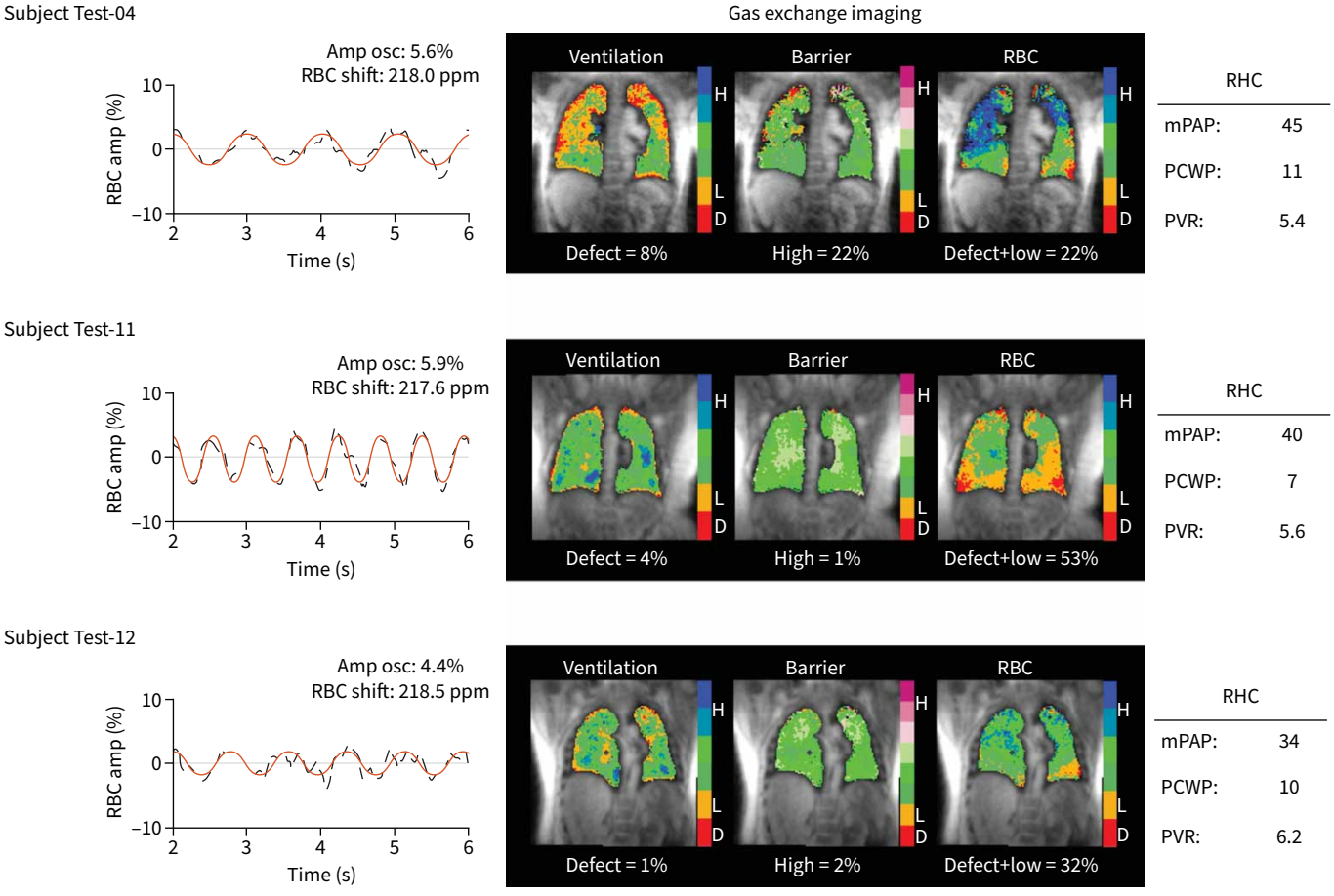

FIGURE 3 Three representative subjects that were all classified as pre-capillary pulmonary hypertension by right heart catheterisation (RHC) and by ^{129}Xe gas-exchange magnetic resonance imaging/MR spectroscopy (^{129}Xe MRI/MRS). All subjects have suppressed red blood cell (RBC) amplitude oscillations and preserved chemical shift on MRS. Gas-exchange imaging reveals that Subject Test-04 has some regions of low ventilation but no extreme ventilation defects, while the remaining subjects have normal ventilation patterns. None of the subjects have high barrier uptake. All three subjects exhibit moderate RBC transfer impairment as indicated by RBC defect+low. amp osc: amplitude oscillations; RHC: right heart catheterisation; mPAP: mean pulmonary artery pressure; PCWP: pulmonary capillary wedge pressure; PVR: pulmonary vascular resistance.

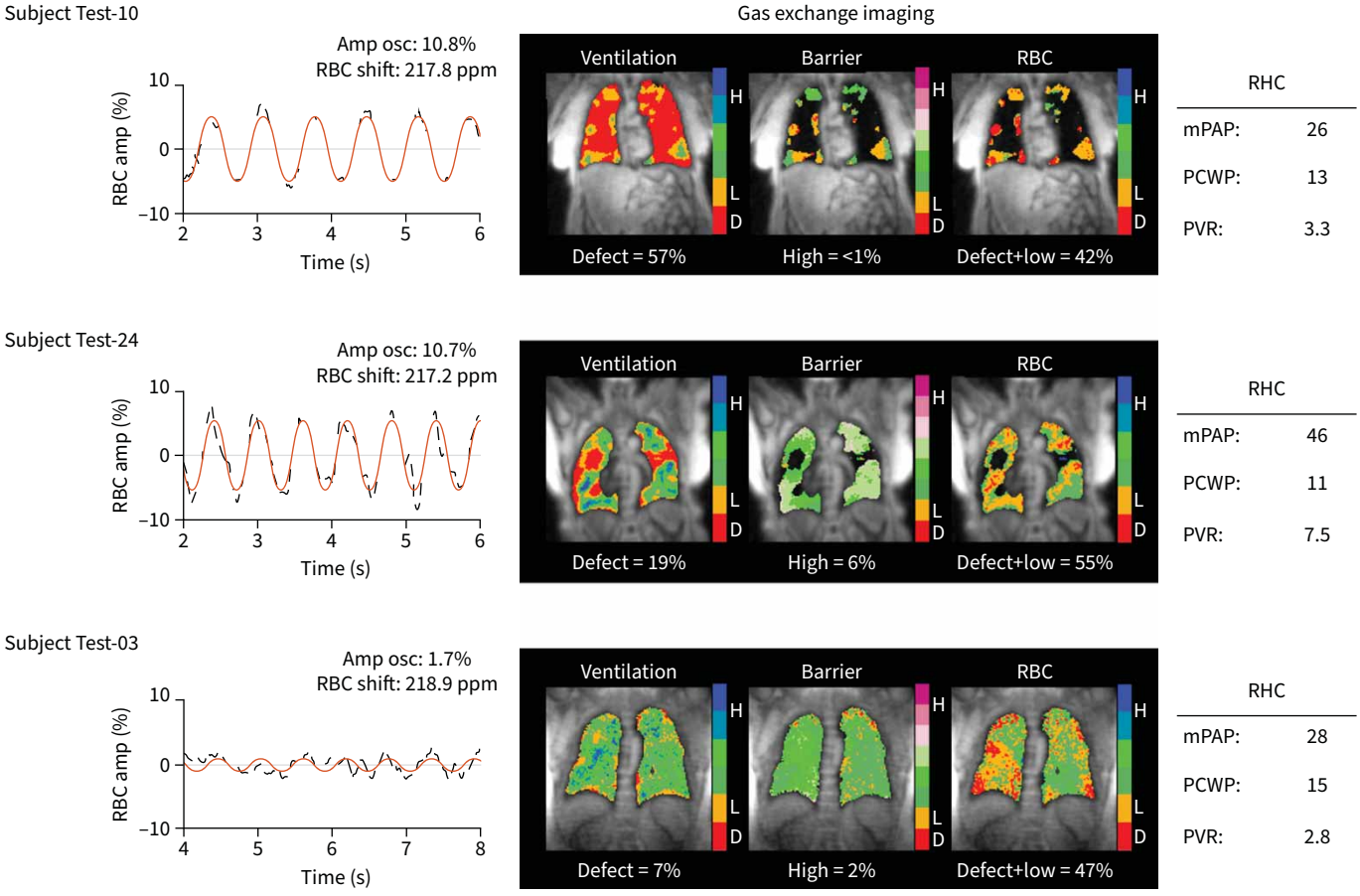

FIGURE 4 Three representative subjects misclassified by ^{129}Xe gas-exchange magnetic resonance imaging/MR spectroscopy (^{129}Xe MRI/MRS). Subject Test-10 has normal red blood cell (RBC) amplitude oscillations with severe ventilation defects indicative of COPD. The subject was classified by ^{129}Xe MRI/MRS as no pulmonary hypertension (PH), but right heart catheterisation (RHC) indicated pre-capillary PH. This may represent proportionate disease. Similarly, Subject Test-24 has normal RBC amplitude oscillations with large ventilation defects from asthma and was classified by ^{129}Xe MRI/MRS as no PH, while RHC indicated pre-capillary PH. Subject Test-03 has very small RBC amplitude oscillations and a high RBC defect+low. ^{129}Xe MRI/MRS indicates pre-capillary PH; however, RHC shows the subject has PH that is neither pre- nor post-capillary. amp osc: amplitude oscillations; mPAP: mean pulmonary artery pressure; PCWP: pulmonary capillary wedge pressure; PVR: pulmonary vascular resistance.

The ^{129}Xe MRI/MRS algorithm evaluated here had modestly high diagnostic accuracy in every classification. The single largest population in the test cohort was pre-capillary PH with over half of the 32 presenting with either pre-capillary or CpcPH. For this group, the diagnostic algorithm provided high specificity and PPV resulting from few false positives, indicating that subjects who exhibit small RBC amplitude oscillations were likely to have pre-capillary PH. However, the lower sensitivity and NPV values indicate a higher rate of false negatives, as not all subjects with pre-capillary PH will exhibit RBC amplitude oscillations below the 8.6% threshold.

The diagnostic algorithm had exceptionally low sensitivities for identifying pure IpcPH (54%) or ILD without PH (29%). However, when IpcPH and ILD were combined into a single classification, the sensitivity increased to 76%. This indicates that ^{129}Xe MRI/MRS can detect the change in pathophysiology responsible for high RBC oscillations seen in these conditions, but additional criteria are needed to enable differentiations of these pathologies. For example, we have since observed that subjects earlier in their ILD disease course or with nonspecific interstitial pneumonia [22] have a more preserved chemical shift. This suggests that the cut-off of RBC chemical shift may have been too restrictive in the current model. These findings demonstrate limitations of the diagnostic algorithm based on a training set of 93 subjects.

While the majority of subjects with post-capillary PH in the training cohort were classified as Group 2 PH, it is worth mentioning that two subjects in our training cohort were found after lung transplant to have

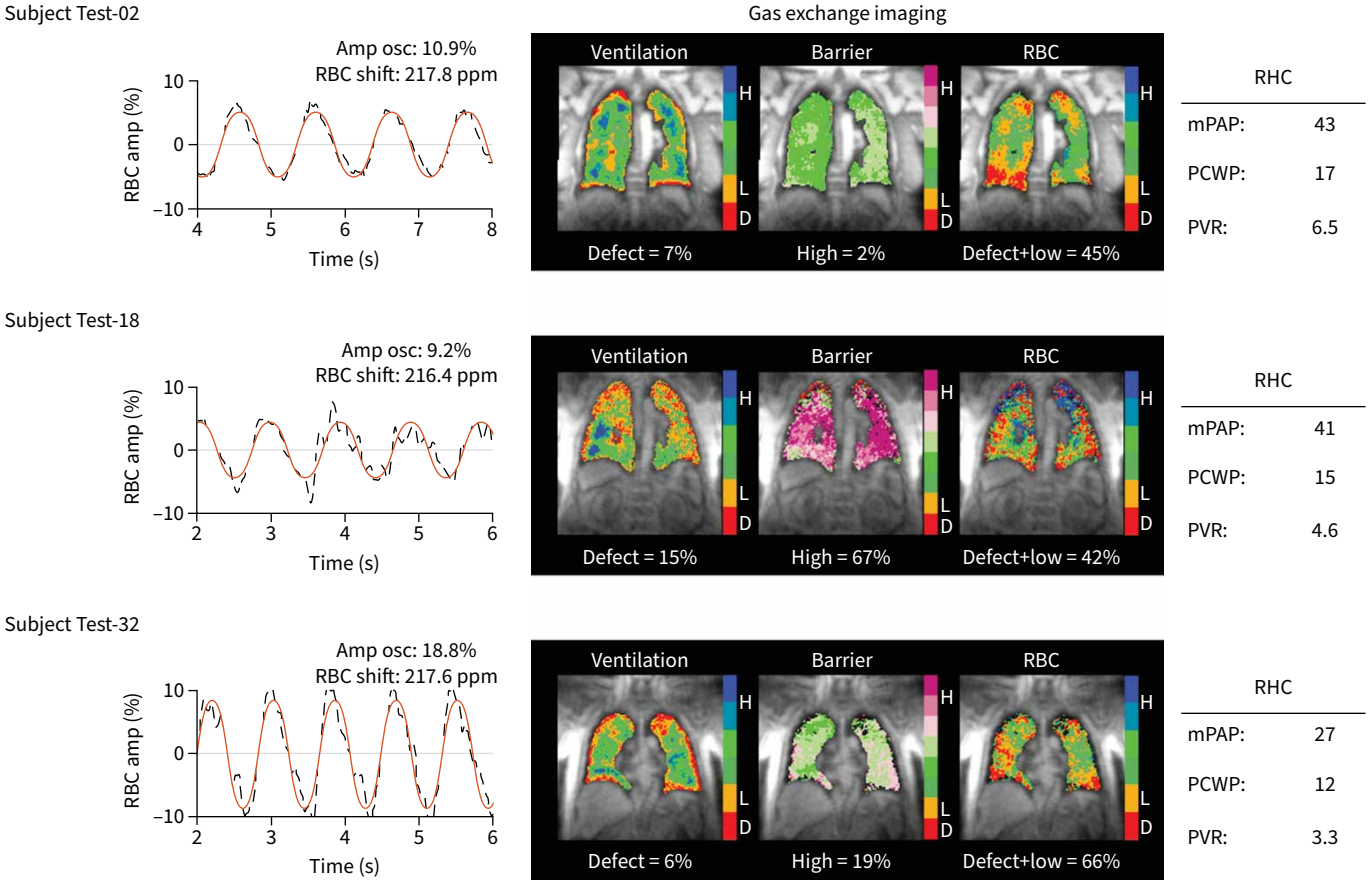

FIGURE 5 Three representative subjects with mixed disease that were misclassified by ^{129}Xe gas-exchange magnetic resonance imaging/MR spectroscopy (^{129}Xe MRI/MRS). Subject Test-02 has normal red blood cell (RBC) amplitude oscillations, but right heart catheterisation (RHC) reveals the subject has combined pre- and post-capillary PH (CpcPH). Subject Test-18 also has normal oscillations with a high barrier uptake that suggests interstitial lung disease (ILD), while RHC reveals pre-capillary PH. These two subjects may represent cases where two competing processes, one that suppresses and one that enhances RBC amplitude oscillations, result in a normal amplitude. Subject Test-32 has high RBC amplitude oscillations, while RHC again indicates pre-capillary PH. This may be proportionate disease. amp osc: amplitude oscillations; mPAP: mean pulmonary artery pressure; PCWP: pulmonary capillary wedge pressure; PVR: pulmonary vascular resistance.

pulmonary veno-occlusive disease (PVOD). It is noteworthy that both subjects presented with high RBC oscillations, minimal ventilation defects, significant RBC transfer defects and a preserved RBC chemical shift. Clinically, the diagnosis of PVOD is particularly challenging, and ^{129}Xe MRI/MRS may ultimately become a valuable tool for identifying this condition.

There were a number of cases in which ^{129}Xe MRI/MRS provided important context to the haemodynamics measured by RHC. The challenges imposed by strict RHC cut-offs are illustrated by the results in figure 4, showing three subjects with PH as defined by RHC, but technically misclassified by the diagnostic algorithm. However, each of these subjects exhibited additional complex disease processes that cannot be quantified by haemodynamic measurements alone. While RHC helps stratify subjects into pre- and/or post-capillary PH, PH is a multifactorial disease, and the simplicity of the RHC classifications obscure the heterogeneity of disease present in an individual subject. Thus, even in cases such as these where ^{129}Xe MRI/MRS appears discordant with the gold standard of RHC, the ability of ^{129}Xe MRI/MRS to noninvasively assess both haemodynamics and visualise gas-exchange impairments may provide the clinician with a more comprehensive assessment of disease.

A major limitation of this diagnostic model is that it only allowed for four mutually exclusive classifications. Thus, in its current form, it cannot be used to detect CpcPH or to confidently detect PH in the presence of ILD. The classification of CpcPH by ^{129}Xe MRS is challenging because pre-capillary PH is expected to suppress RBC oscillations while post-capillary PH should enhance them, resulting in a mixture of suppressed and enhanced oscillations that, when averaged over the entire lung, can easily cancel

to yield RBC amplitude oscillations in the healthy reference range. Similarly, for subjects with pre-capillary PH in the presence of ILD, the model cannot separate the two competing processes of enhanced and suppressed oscillations. Ultimately, such cases may be better analysed by employing the recently developed method that allows RBC oscillations to be imaged [32]. Such an approach can spatially localise regions of high and low oscillations to separately visualise the presence of both processes. However, this method requires higher image SNR than was consistently available at the time this dataset was obtained and would thus have to be incorporated prospectively in future trial designs.

Our study had a number of other limitations. First was the relatively small training cohort from which the algorithm was derived, along with the low prevalence of IpcPH, no PH and no ILD, and ILD. Moreover, while the test cohort was exclusively scanned at 3 T, the training cohort contained ^{129}Xe MRI/MRS studies performed at both 1.5 T and 3 T. While no significant difference has been found between the gas-exchange mapping or spectroscopy results at the two field strengths [33], it is possible that algorithm performance is sensitive to field strength. Another important source of variation could be differences in lung inflation levels. Higher lung inflation reduces both the barrier and RBC signals relative to the gas signal and likely affects the RBC oscillations heights. Although patients were coached to inhale the ^{129}Xe dose from functional residual capacity, it is possible that they did not reliably reach their target expiratory or inspiratory lung volumes.

Additionally, our test population was inherently biased since only patients that had already been referred to RHC were recruited for this study and thus resulted in an uneven distribution of subjects across PH states. Furthermore, not all patients underwent RHC on the same day, which increased the potential variability in pathophysiology between the time of RHC and ^{129}Xe MRI/MRS. This study did not explore ^{129}Xe MRI/MRS in subjects with current illness with lung involvement and thus cannot be used in subjects with concomitant infection. Future studies should include an external validation cohort to validate the utility of the diagnostic algorithm in multicenter studies. A larger test cohort will also provide the opportunity to explore the relationship between ^{129}Xe MRI/MRS and other clinical measurements, including RHC, echocardiography and cardiac MR, to better understand the relationship between ^{129}Xe MRI/MRS measurements and disease pathophysiology especially in subjects with concomitant PH and pulmonary disease.

In conclusion, these results suggest that diagnostic models based on ^{129}Xe MRI/MRS metrics can be developed to noninvasively detect pre-capillary PH, IpcPH and ILD. The combination of ^{129}Xe dynamic MRS and imaging provides an assessment of both haemodynamics and gas-exchange impairment for a comprehensive patient evaluation. Weaknesses in the current diagnostic algorithm could be addressed by using a larger training set with a broader range of cardiopulmonary diseases, with explicit inclusion of CpcPH, PH-ILD and PH-COPD populations. Other ^{129}Xe MRI/MRS metrics could also be incorporated, such as oscillation imaging to detect regional variations in pulmonary pressures and increase diagnostic accuracy. Such improvements could allow the development of ^{129}Xe MRI/MRS as a useful tool in the diagnosis of patients with PH.

Acknowledgements: We gratefully acknowledge the selfless contributions of our patients and the tireless commitment of our clinical research coordinators.

Provenance: Submitted article, peer reviewed.

Conflict of interest: E.A. Bier. reports a provisional patent for “Dynamic ^{129}Xe Gas Exchange Spectroscopy.” F. Alenezi. has nothing to disclose. J. Lu. has nothing to disclose. Z. Wang. reports a provisional patent for “Dynamic ^{129}Xe Gas Exchange Spectroscopy.” J.G. Mammarappallil reports consulting fees from Coreline Imaging and Bard Peripheral, and payments from Boehringer Ingelheim for lectures or presentations, outside the submitted work. B. O’Sullivan-Murphy has nothing to disclose. A. Erkanli has nothing to disclose. B. Driehuys reports grants from the National Institutes of Health during the conduct of the study and a provisional patent for “Dynamic ^{129}Xe Gas Exchange Spectroscopy”; and reports personal fees from and is founder and chief technology officer for Polarean Imaging, a company which produces ^{129}Xe hyperpolarisation equipment, outside the submitted work. S. Rajagopal reports grants from the National Institutes of Health and a provisional patent for “Dynamic ^{129}Xe Gas Exchange Spectroscopy”; and reports consulting fees from APIE Therapeutics, Altavant, Gossamer Bio, Insmed, Janssen Pharmaceuticals, Liquidia Technologies, Polarean, United Therapeutics Corp. and Visterra, and payments from TotalCME and AcademicCME for lectures or presentations, outside the submitted work.

Support statement: This study was funded by NIH/NHLBI R01 HL105643, NIH/NHLBI R01HL126771 and HHSN268201700001C. Funding information for this article has been deposited with the Crossref Funder Registry.

References

1 Kruger SJ, Nagle, SK Couch, MJ, *et al.* Functional imaging of the lungs with gas agents. *J Magn Reson Imaging* 2016; 43: 295–315.
2 Grist JT, Chen M, Collier GJ, *et al.* Hyperpolarized ^{129}Xe MRI abnormalities in dyspneic participants 3 months after covid-19 pneumonia: preliminary results. *Radiology* 2021; 301: E353–E360.
3 Collier GJ, Eaden JA, Hughes PJC, *et al.* Dissolved ^{129}Xe lung MRI with four-echo 3D radial spectroscopic imaging: quantification of regional gas transfer in idiopathic pulmonary fibrosis. *Magn Reson Med* 2021; 85: 2622–2633.
4 Cherubini A, Bifone A. Hyperpolarised xenon in biology. *Prog Nucl Magn Reson Spectrosc* 2003; 42: 1–30.
5 Wang Z, He M, Bier E, *et al.* Hyperpolarized ^{129}Xe gas transfer MRI: the transition from 1.5 T to 3 T. *Magn Reson Med* 2018; 80: 2374–2383.
6 Bier EA, Robertson SH, Schrank, GM, *et al.* A protocol for quantifying cardiogenic oscillations in dynamic ^{129}Xe gas exchange spectroscopy: the effects of idiopathic pulmonary fibrosis. *NMR Biomed* 2019; 32: e4029.
7 Ruppert K, Altes TA, Mata JF, *et al.* Detecting pulmonary capillary blood pulsations using hyperpolarized xenon-129 chemical shift saturation recovery (CSSR) MR spectroscopy. *Magn Reson Med* 2016; 75: 1771–1780.
8 Norquay G, Stewart NJ, Wild JM. Evaluation of ^{129}Xe-RBC signal dynamics and chemical shift in the cardiopulmonary circuit using hyperpolarized ^{129}Xe NMR. *Proc Int Soc Magn Reson Med* 2017; 25: 3327.
9 Wang Z, Swaminathan A, Parikh K, *et al.* Diverse cardiopulmonary diseases are associated with distinct xenon magnetic resonance imaging signatures. *Eur Respir J* 2019; 54: 1900831.
10 Galiè N, Vachiery J-L Gibbs S, *et al.* 2015 ESC/ERS guidelines for the diagnosis and treatment of pulmonary hypertension: the joint task force for the diagnosis and treatment of pulmonary hypertension of the European Society of Cardiology (ESC) and the European Respiratory Society (ERS): endorsed by: Association for European Paediatric and Congenital Cardiology (AEPC), International Society for Heart and Lung Transplantation (ISHLT). *Eur Heart J* 2016; 37: 67–119.
11 Vachiéry J-L, Gaine S. Challenges in the diagnosis and treatment of pulmonary arterial hypertension. *Eur Respir Rev* 2012; 21: 313–320.
12 Galiè N, Hoeper MM, Humbert M, *et al.* Guidelines for the diagnosis and treatment of pulmonary hypertension: the Task Force for the Diagnosis and Treatment of Pulmonary Hypertension of the European Society of Cardiology (ESC) and the European Respiratory Society (ERS), endorsed by the International Society of Heart and Lung Transplantation (ISHLT). *Eur Heart J* 2009; 30: 2493–2537.
13 Kovacs G, Berghold A, Scheidl S, *et al.* Pulmonary arterial pressure during rest and exercise in healthy subjects: a systematic review. *Eur Respir J* 2009; 34: 888–894.
14 Wang JM, Robertson SH, Wang Z, *et al.* Using hyperpolarized ^{129}Xe MRI to quantify regional gas transfer in idiopathic pulmonary fibrosis. *Thorax* 2018; 73: 21–28.
15 Wang Z, Robertson SH, Wang J, *et al.* Quantitative analysis of hyperpolarized ^{129}Xe gas transfer MRI. *Med Phys* 2017; 44: 2415–2428.
16 He M, Robertson SH, Kaushik SS, *et al.* Dose and pulse sequence considerations for hyperpolarized 129 Xe ventilation MRI. *Magn Reson Imaging* 2015; 33: 877–885.
17 Niedbalski PJ, Hall CS, Castro M, *et al.* Protocols for multi-site trials using hyperpolarized ^{129}Xe MRI for imaging of ventilation, alveolar-airspace size, and gas exchange: a position paper from the ^{129}Xe MRI clinical trials consortium. *Magn Reson Med* 2021; 86: 2966–2986.
18 Ruppert K, Amzajerdian F, Hamedani H, *et al.* Assessment of flip angle–TR equivalence for standardized dissolved-phase imaging of the lung with hyperpolarized ^{129}Xe MRI. *Magn Reson Med* 2019; 81: 1784–1794.
19 Kaushik SS, Robertson SH, Freeman MS, *et al.* Single-breath clinical imaging of hyperpolarized ^{129}Xe in the airspaces, barrier, and red blood cells using an interleaved 3D radial 1-point Dixon acquisition. *Magn Reson Med* 2016; 75: 1434–1443.
20 SAS Institute Inc. JMP 15 Predictive and Specialized Modeling. : Cary, NC, SAS Institute, 2019.
21 Hastie TJ, Tibshirani RJ, Friedman JH. The Elements of Statistical Learning: Data Mining, Inference, and Prediction. 2nd Edn. New York, Springer-Verlag, 2009.
22 Mummy DG, Bier EA, Wang Z, *et al.* Hyperpolarized 129 Xe MRI and spectroscopy of gas-exchange abnormalities in nonspecific interstitial pneumonia. *Radiology* 2021; 301: 211–220.
23 Rankine LJ, Wang Z, Wang JM, *et al.* ^{129}Xenon gas exchange magnetic resonance imaging as a potential prognostic marker for progression of idiopathic pulmonary fibrosis. *Ann Am Thorac Soc* 2020; 17: 121–125.
24 Simonneau G, Celermajer DS, Denton CP, *et al.* Haemodynamic definitions and updated clinical classification of pulmonary hypertension. *Eur Respir J* 2019; 53: 1801913.
25 Rosenkranz S, Blindt R, Bonderman D, *et al.* Pulmonary hypertension associated with left heart disease: Updated Recommendations of the Cologne Consensus Conference 2018. *Int J Cardiol* 2018; 272: 53–62.
26 Maron BA, Brittain EL, Hess E, *et al.* Pulmonary vascular resistance and clinical outcomes in patients with pulmonary hypertension: a retrospective cohort study. *Lancet Respir Med* 2020; 8: 873–884.
27 Farha S, Su Q, Yamaji-Kegan K, *et al.* Loss of alveolar membrane diffusing capacity and pulmonary capillary blood volume in pulmonary arterial hypertension. *Respir Res* 2013; 14: 1–8.

28 Godinas L, Amar D, Montani D, *et al.* Lung capillary blood volume and membrane diffusion in precapillary pulmonary hypertension. *J Heart Lung Transplant* 2016; 35: 647–656.

29 Hoeper MM, Bogaard HJ, Condliffe R, *et al.* Definitions and diagnosis of pulmonary hypertension. *J Am Coll Cardiol* 2013; 62: D42–D50.

30 Maron BA, Abman SH, Elliott CG, *et al.* Pulmonary arterial hypertension: diagnosis, treatment, and novel advances. *Am J Respir Crit Care Med* 2021; 203: 1472–1487.

31 Janda S, Shahidi N, Gin K, *et al.* Diagnostic accuracy of echocardiography for pulmonary hypertension: a systematic review and meta-analysis. *Heart* 2011; 97: 612–622.

32 Niedbalski PJ, Willmering MM, Robertson, SH, *et al.* Mapping and correcting hyperpolarized magnetization decay with radial keyhole imaging. *Magn Reson Med* 2019; 82: 367–376.

33 Wang Z, He M, Virgincar R, *et al.* Quantifying hyperpolarized ^{129}Xe gas exchange MRI across platforms, field strength, and acquisition parameters. In International Society for Magnetic Resonance in Medicine 27th Annual Meeting, 11–16 May 2019, Montreal, Canada, p. 6608.